

# SIMULATING REACTIVE/PASSIVE POSTURES BY MEANS OF A HUMAN ACTIVE TORQUE HYBRID MINIMIZATION

I. Rodríguez

*Department of Applied Mathematics and Analysis, University of Barcelona, Barcelona, Spain  
inma@maia.ub.es*

R. Boulic

*Virtual Reality Lab., Ecole Polytechnique Fédérale de Lausanne, Switzerland  
ronan.boulic@epfl.ch*

Keywords: virtual human poses, active muscle torque, passive resistive torque

Abstract: In this paper we propose a hybrid approach minimizing the active torque produced by muscles groups at the joint level. The proposed approach is hybrid in the sense that it combines the local knowledge of the external torque induced by external forces such as gravity and exerted force, and the full knowledge of the passive-resistive torque characteristics due to ligaments and connective tissues. The algorithm is exploited within a context of posture adjustment when a muscle group reaches a critical fatigue level. It proposes a target joint state that can be characterized as active or passive. The active solution, if it exists, can be further characterized by a desired degree of active torque amplitude reduction (between 0 and 100%). In any cases at least one passive solution exists; it relies on the passive/resistive torque appearing in the neighbourhood of the joint limits.

## 1 INTRODUCTION

Postures and motions generated by the human body are very difficult to simulate since it has so many interrelated muscles that produce movement. Muscles contractions are directly influenced by physiological factors such as fatigue or psychological factors such as the state of mind. Biomechanical and biomedical studies have modelled some of these factors (Kulig et al., 1984) (Kumar, 1986). In Computer Animation, Multon proposed a simulation environment where biomechanicians could experiment on the motion dynamics of a virtual arm (Multon, 1998). Komura combined Delp's musculoskeletal model (Delp, 1990) and Giat's fatigue model (Giat et al., 1993) to deal with full body character animations (Komura et al. 2001).

The present paper is complementary to prior studies in computer animation in the sense that we investigate, at the joint level, how to reduce the active torque as a function of an active or a passive strategy. Indeed, this factor strongly influences the

postures adopted by individuals leading to reactive or relaxed postures as recalled now. Early studies showed that people resting with no immediate action to do, tended to adopt asymmetrical (left/right body side bears body weight) poses such as the pelvic slouch (Evans, 1979). An asymmetrical posture is a relaxed pose, incompatible with sudden responses. For example, people waiting to be collected or waiting for the bus. If there is a possibility of having to do something, people adopt a symmetrical standing (standing people such as police officers, waiters, etc.). In an asymmetrical stance, the knee of the supporting limb is fully extended and the thigh fully adducted, therefore knee and hip joints finish up hanging on their ligaments which produce passive moment. This is also known as the *contraposto* posture in sculpture (e.g. "David" of Michelangelo).

Our hypothesis is that active torque, produced by the muscle activation, can be reduced by means of two strategies: either an *active* strategy searching for a solution while staying in the mid-range of the joint where the muscle efficiency is the highest, or a *passive* one searching for the always existing

passive-resistive solution that compensates the external torque in the neighborhood of the joint limits. Considering these strategies allows to generate a larger space of realistic postural solutions; the active strategy achieves *reactive* poses while the passive one produces *relaxed* poses.

The paper presents an initial evaluation of a general algorithm of hybrid minimization of the active torque under the quasi-static hypothesis. It is illustrated on a simple case study (i.e. the elbow joint) to characterize the various convergence configurations arising from its specificity of exploiting the local knowledge of the external torque and the full knowledge of the passive torque behavior.

## 2 ACTIVE TORQUE REDUCTION SCHEME

Under the quasi-static hypothesis, the sum of all torques is null for all joints. Therefore the joint active torque  $\tau_a$  can be expressed as follows:

$$\tau_a = -(\tau_p + \tau_e) \quad (1)$$

where,  $\tau_p$  and  $\tau_e$  represent, respectively, the current passive and external joint torques. The external torque  $\tau_e$  is produced by gravity and any other external forces, while the passive torque  $\tau_p$  is due to the resistance of the joint surrounding tissues (ligaments and connective tissues) to be extended or compressed. A null active torque is achieved when:

$$\tau_e = -\tau_p \quad (2)$$

This is illustrated on Figure 1 where we have three postures (photos) with a null active torque for the elbow joint.

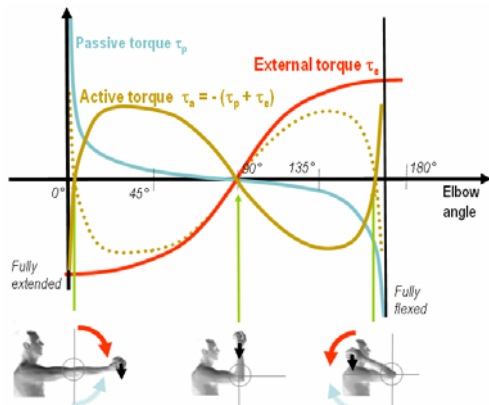


Figure 1: Frontal elbow case study highlighting the passive torque (blue), the external torque (red), resulting

active torque (brown) and minus active torque (dotted brown) under the quasi-static hypothesis. In this case, only the elbow joint is varying.

### 2.1 Muscle action strategy

Our system introduces the muscle action strategy in order to determine the influence of passive/resistive torque (Hatze, 1997) in the active torque reduction process.

An *active* strategy strives to find a solution close to the mid-range of the joint where the muscle group is efficient to produce its active torque,  $\tau_a$ . Such a region can be also characterized by a quasi-null passive resistive torque ( $\tau_p \approx 0$ , see Figure 1).

The *passive* strategy only exploits the joint passive torque to compensate the action of the external torque. Such a solution is always in the neighborhood of the joint limits, resulting in less reactive/responsive muscles groups because muscles forces are small even for a high degree of activation.

In the scenario from Figure 1, only the elbow joint is allowed to move. Three postures with a null active torque are highlighted (with a photo below). The one in the central joint range is the *active* solution as it maximizes the muscle activation efficiency while the other two are purely passive/resistive, hence less responsive.

### 2.2 Hybrid algorithm

The proposed approach is hybrid in the sense that it combines the *local* knowledge of the external torque  $\tau_e$  and the *full* knowledge of the passive-resistive torque characteristics  $\tau_p$ .

Indeed, in the general case, the number of considered joints can be arbitrary large leading to unknown variation of the external torque at the individual joint level. In the quasi-static context we can simply evaluate its current value  $\tau_e$ , by means of the principle of the virtual works (Craig, 1986) and its current first derivative,  $d\tau_e$  (section 3). As a direct consequence, the algorithm we propose exploits only a linear extrapolation of the external torque based on this information.

On the other hand, we assume we know the passive torque function  $\tau_p$  over the full joint range from the Biomechanics literature (Esteki and Mansour, 1996).

As a side remark, in the use-cases illustrating the paper (Figure 1, Figure 10, Figure 12), the external torque is induced by the gravity, and the only joint that moves is the elbow. This allows to draw the external torque function (i.e. the red curve); however

only the local knowledge of the external torque is exploited in the result section.

In addition to the specification of the strategy type - *active vs passive* - the active strategy selects its solution based on a normalized quantity called the *active torque decrease ratio*  $R$  characterizing the quality of the optimized active torque. We have:

$$R = (\tau_a - \tau_{a\_min}) / \tau_a \quad (3)$$

where  $\tau_a$  represents the current active torque,  $\tau_{a\_min}$  is the estimated local minimum of the active torque amplitude, when it exists, in addition to the null global minima achieved with the passive strategy.

When  $\tau_{a\_min}$  is null, a 100% of  $\tau_a$  decrease ratio is achieved. This is the ideal case. In other less optimal cases smaller values of  $R$  are achieved. For this reason, the active strategy accepts a threshold level  $R_{min}$  on this quantity (potentially user-defined). Whenever  $R$  is smaller than  $R_{min}$  then the solution provided by the active strategy is not accepted and the algorithm switches to the always-existing extremal passive solution. For example, a  $R_{min}$  value of 0.9 means that the user agrees to have down to only 90% compensation because the remaining 10% of active torque is a bearable amplitude. This favors solutions lying in the mid joint range characterizing a more reactive posture, even if they are not fully optimal in terms of amplitude.

Table 1 details the algorithm providing the angle  $\theta_g$  with reduced active torque. Its input is the current joint state  $\theta_c$ , the *active* strategy boolean, the current values of  $\tau_c$ ,  $\tau_p$  and  $\tau_a$ , the current first derivative of the external torque  $d\tau_c$  and of the passive torque  $d\tau_p$  (tabulated), and the threshold  $R_{min}$ .

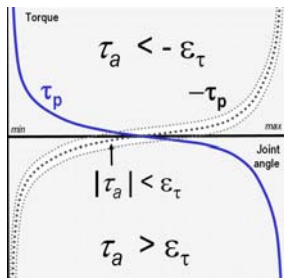


Figure 2: Sign of  $\tau_a$  with equality tolerance  $\epsilon_\tau$

The following constants or precomputed information are useful for the algorithm too:

$\theta_{d\tau_p}(d\tau_p)$ : given the slope of the external torque  $d\tau_c$ , this function searches for the angle(s) where  $d\tau_p = -d\tau_c$ .

$d\tau_{p\_min}$ : smallest passive torque slope (absolute value).

$\theta_{d\tau_p\_min}$ : joint angle for which  $d\tau_p = d\tau_{p\_min}$ .

$\theta_{s\_min}, \theta_{s\_max}$ : pair of angle values on both sides of  $\theta_{d\tau_p\_min}$  for which  $d\tau_p = -d\tau_c$ .

$\epsilon_\tau$ : equality tolerance for  $\tau_c = -\tau_p$ .

Two useful temporary variables are:

$\tau_{a\_min}$ : value of the estimated  $\tau_a$  minima.

$\theta_{\tau_a\_min}$ : if  $(\tau_a > 0) \theta_{\tau_a\_min} = \theta_{s\_max}$  else  $\theta_{\tau_a\_min} = \theta_{s\_min}$ .

In addition, the `Dichotomy` function allows to find the goal angle where the extrapolated external torque line intersects with the opposite of the passive torque function (dotted curve in Figure 2). Two variants of searching DSS and DOS are detailed in table2.

```

Search slopes for  $\theta_{d\tau_p}(-d\tau_c)$ 
if no or only one slope
{ if ( $|\tau_a| < \epsilon_\tau$ )  $\theta_g := \theta_c$  // CASE 1.1
  else if ( $\tau_a > \epsilon_\tau$ )
     $\theta_g := \text{Dichotomy}(\theta_{min}, \theta_c, \theta_g)$  // CASE 1.2
  else
     $\theta_g := \text{Dichotomy}(\theta_c, \theta_{max}, \theta_g)$  // CASE 1.3
}
else // two slopes
{ if ( $|\tau_a| < \epsilon_\tau$ )
  { if ( ( $\theta_{s\_min} < \theta_c < \theta_{s\_max}$ ) or
    [ ( $\theta_c < \theta_{s\_min}$  OR  $\theta_c > \theta_{s\_max}$ )
    and ( $\text{sign}(\tau_a(\theta_{s\_min})) = \text{sign}(\tau_a(\theta_{s\_max}))$ ) ] )
     $\theta_g := \theta_c$  // CASE 2.1
  else
    { if (active) // CASE 2.2
       $\text{Dichotomy}(\theta_{s\_min}, \theta_{s\_max}, \theta_g)$ 
    else  $\theta_g := \theta_c$  // CASE 2.3
    }
}
} else //  $|\tau_a| > \epsilon_\tau$ 
{ if (  $\text{sign}(\tau_a) = \text{sign}(\tau_a(\theta_{s\_min}))$ 
  and  $\text{sign}(\tau_a) = \text{sign}(\tau_a(\theta_{s\_max}))$  )
  { if (active AND ( $(\tau_a - \tau_a(\theta_{\tau_a\_min})) / \tau_a > R_{min}$ ))
     $\theta_g := \theta_{\tau_a\_min}$  // CASE 3.1
  else // CASE 3.2
     $\theta_g := \text{DSS}(\tau_a, \theta_{min}, \theta_{max}, \theta_{s\_min}, \theta_{s\_max})$ 
  }
} else
{ if (active) // CASE 3.3
   $\theta_g := \text{Dichotomy}(\theta_{s\_min}, \theta_{s\_max})$ 
  else // CASE 3.4
     $\theta_g := \text{DOS}(\tau_a, \theta_c, \theta_{min}, \theta_{max}, \theta_{s\_min}, \theta_{s\_max})$ 
} } }

```

Table 1. Minimum active torque search

<pre> DSS(<math>\tau_a, \theta_{\min}, \theta_{\max}, \theta_{s_{\min}}, \theta_{s_{\max}}</math>) := Dichotomy( SameSignMinandMax(<math>\tau_a, \theta_{\min}, \theta_{\max}, \theta_{s_{\min}}, \theta_{s_{\max}}</math>), <math>\theta_g</math> ) SameSignMinandMax(input: <math>\tau_a, \theta_{\min}, \theta_{\max}, \theta_{s_{\min}}, \theta_{s_{\max}}</math>, output: SameSignMin, SameSignMax) {   if(<math>\tau_a &gt; \epsilon_\tau</math>) // <math>\tau_e</math> is below the curve <math>-\tau_p(\theta)</math>   { SameSignMin := <math>\theta_{\min}</math>, SameSignMax := <math>\theta_{s_{\min}}</math> }   else // <math>\tau_e</math> is above the curve <math>-\tau_p(\theta)</math>   { SameSignMin := <math>\theta_{s_{\max}}</math>, SameSignMax := <math>\theta_{\max}</math> } } </pre>
<pre> DOS(<math>\tau_a, \theta_c, \theta_{\min}, \theta_{\max}, \theta_{s_{\min}}, \theta_{s_{\max}}</math>) := Dichotomy( OppoSgnMinandMax(<math>\tau_a, \theta_c, \theta_{\min}, \theta_{\max}, \theta_{s_{\min}}, \theta_{s_{\max}}</math>), <math>\theta_g</math> ) OppoSgnMinandMax (input : <math>\tau_a, \theta_c, \theta_{\min}, \theta_{\max}, \theta_{s_{\min}}, \theta_{s_{\max}}</math> output: OppoSgnMin, OppoSgnMax) {   if(<math>\tau_a &gt; \epsilon_\tau</math>) // <math>\tau_e</math> is below the curve <math>-\tau_p(\theta)</math>    if( <math>\theta_c &lt; \theta_{s_{\max}}</math> ) { OppoSgnMin := <math>\theta_{\min}</math>, OppoSgnMax := <math>\theta_{s_{\min}}</math> }   else { OppoSgnMin := <math>\theta_{s_{\max}}</math>, OppoSgnMax := <math>\theta_{\max}</math> } } else // <math>\tau_e</math> is above the curve <math>-\tau_p(\theta)</math> {   if( <math>\theta_c &gt; \theta_{s_{\min}}</math> ) { OppoSgnMin := <math>\theta_{s_{\max}}</math>, OppoSgnMax := <math>\theta_{\max}</math> }   else { OppoSgnMin := <math>\theta_{\min}</math>, OppoSgnMax := <math>\theta_{s_{\min}}</math> } } } </pre>

Table 2. Functions defining intervals of dichotomic search (general algorithm-cases 3.2 and 3.4)

The following figures illustrate the different cases of the hybrid minimization. Figure 3a is a case where no active solution can be found as no slope in the function  $-\tau_p$  matches  $d\tau_e$ . A passive solution is found by dichotomy (intersection of the external torque line with the opposite of the passive torque function). In Figure 3b the current state is already optimal.

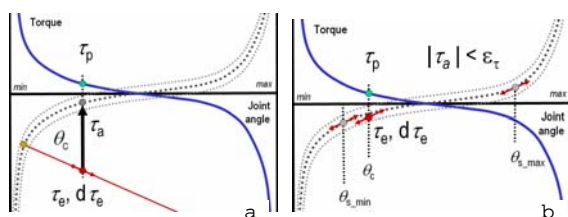


Figure 3: (a) **CASE 1.2**: no slope in  $-\tau_p$  matching  $d\tau_e$ , (b) **CASE 2.1**:  $|\tau_a| < \epsilon_\tau$  and  $(\theta_{s_{\min}} < \theta_c < \theta_{s_{\max}})$

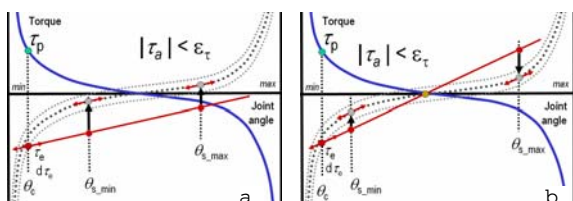


Figure 4: (a) **CASE 2.1**:  $|\tau_a| < \epsilon_\tau$  and  $(\theta_c < \theta_{s_{\min}}$  or  $\theta_c > \theta_{s_{\max}})$  and  $(\text{sign}(\tau_a(\theta_{s_{\min}})) = \text{sign}(\tau_a(\theta_{s_{\max}})))$ , (b) **CASE 2.2, CASE 2.3**:  $|\tau_a| < \epsilon_\tau$  and  $(\theta_c < \theta_{s_{\min}}$  or  $\theta_c > \theta_{s_{\max}})$  and  $(\text{sign}(\tau_a(\theta_{s_{\min}})) \neq \text{sign}(\tau_a(\theta_{s_{\max}})))$ ,

In Figure 4 the current state belongs to the equality approximation but this time the joint angle is smaller than  $\theta_{s_{\min}}$ , hence one more sign test is required to determine whether another joint angle, closer to the mid-range, exists. One is found only in

Figure 4b because the active torque changes sign between  $\theta_{s_{\min}}$  and  $\theta_{s_{\max}}$ , while this is not the case for Figure 4a.

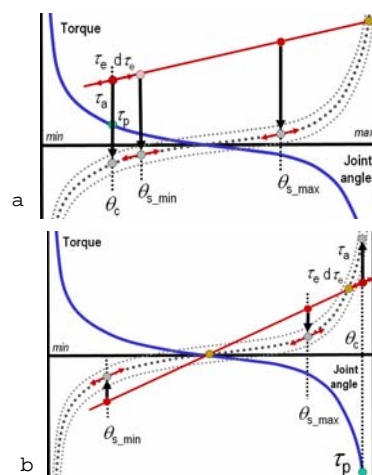


Figure 5: (a) **CASE 3.1, CASE 3.2**:  $|\tau_a| > \epsilon$  and  $(\text{sign}(\tau_a) = \text{sign}(\tau_a(\theta_{s_{\min}})))$  and  $(\text{sign}(\tau_a) = \text{sign}(\tau_a(\theta_{s_{\max}})))$ , (b) **CASE 3.3 or 3.4**:  $|\tau_a| > \epsilon$  and  $(\text{sign}(\tau_a) \neq \text{sign}(\tau_a(\theta_{s_{\min}})))$  or  $(\text{sign}(\tau_a) \neq \text{sign}(\tau_a(\theta_{s_{\max}})))$

Figure 5 illustrates cases where the current active torque is not null (e.g. a downward black arrow indicates a negative value). In Figure 5a the two angles  $\theta_{s_{\min}}$  and  $\theta_{s_{\max}}$ , with the same slope as  $d\tau_e$  indicate extrema of the active torque variation (with constant sign), the minimum amplitude being obtained for  $\theta_{s_{\min}}$ . In Figure 5b the active torque changes sign between  $\theta_{s_{\min}}$  and  $\theta_{s_{\max}}$ . If the strategy is active a search is conducted within this interval, otherwise the closest solution is found.

### 3 ALGORITHM EXPLOITATION

The reduced active torque algorithm is exploited, within a context of posture adjustment, by means of an Inverse Kinematics engine (Baerlocher et al., 2004). When a muscle group reaches critical fatigue levels (Rodríguez, 2004), the active torque reduction algorithm proposes a target joint angle reducing the active torque, hence the fatigue too.

In our fatigue reduction scheme we enforce a hard linear inequality constraint whenever the active torque amplitude of a fatigued joint  $i$  has to be reduced:

$$a_i^T \boldsymbol{\theta} \leq b_i \quad (4)$$

where  $\boldsymbol{\theta}$  represents the  $n$ -dimensional vector of joint coordinates,  $a_i$  is the  $n$ -dimensional gradient vector of the inequality constraint hyperplane and  $b_i$  is a scalar. Figure 6 illustrates the construction of one inequality constraint in 2D, the current configuration  $\boldsymbol{\theta}$  is out of the feasible region, requesting a  $\Delta\boldsymbol{\theta}$  to drive it to the feasible region. This variation vector has an opposite direction to the *constraint gradient* vector  $a^T$ :

$$a^T = -\text{normalized}(\Delta\boldsymbol{\theta}) \quad (5)$$

The scalar product of  $a^T$  with any  $\theta_H$  lying on the hyperplane, such as  $\theta + \Delta\theta$ , gives the scalar  $b$ :

$$b = a^T \boldsymbol{\theta}_H \quad (6)$$

We have all the elements, as shown in formula (4), that define a fatigue reduction inequality constraint for guiding a posture from an unfeasible region to a feasible one.

In the following we describe how the joint variation  $\Delta\boldsymbol{\theta}$  has to be computed in order to adjust the posture leading to a minimization of active torque and therefore to a less fatigued posture.

The vector  $J\tau_{el}$  gathers the partial derivatives of its external torque  $\tau_{el}$  with respect to all joints:

$$J\tau_{el} = \left\{ \begin{array}{c} \delta\tau_{el} \\ \delta\theta_j \end{array} \right\}_{j=1,n} \quad (7)$$

Its scalar component  $\delta\tau_{el}/\delta\theta_l$  for the fatigued joint  $l$  is the constant external torque derivative  $d\tau_e$  used in the general algorithm from Table 1.

To compute  $J\tau_{el}$ , we need the Jacobians  $J_{Tl}$  associated with the external forces  $f_i$  and the gravity

Jacobian  $J_G$  associated with the weight  $w$ . This is the expression of the partial derivative corresponding to joint  $j$ :

$$\frac{\delta\tau_{el}}{\delta\theta_j} = \sum_i^{ne} J_{Tl_i} \cdot (f_i \times r_j) + J_{G_l} \cdot (w \times r_j) \quad (8)$$

where  $ne$  is the number of external forces,  $J_{Tl_i}$  is the column  $l$  of  $J_{Tl}$ ,  $J_{G_l}$  is the column  $l$  of  $J_G$  associated with the weight  $w$ , and  $r_j$  represents the unit axis of rotation of joint  $j$ .

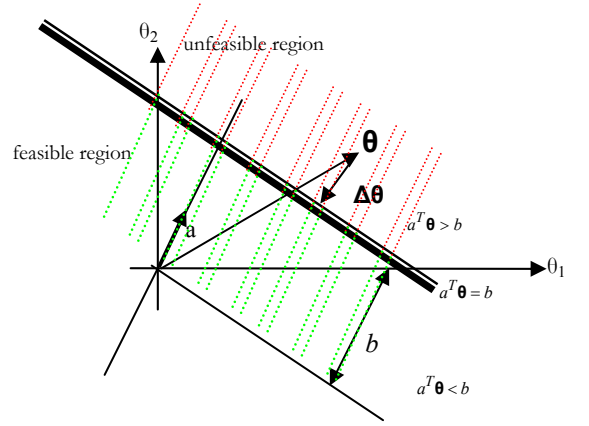


Figure 6. Example of hyperplane in 2D

The general algorithm presented in Table 1 exploits the scalar component  $d\tau_e$  corresponding to  $\delta\tau_{el}/\delta\theta_l$ . It proposes a target joint angle  $\theta_g$  used to build the component  $l$  of the posture variation  $\Delta\boldsymbol{\theta}$  associated to the inequality constraint bringing the posture in the fatigue recovery region:

$$\Delta\theta_l = \min(\beta(\theta_g - \theta_c), \Delta\theta_{max}) \quad (9)$$

where  $\theta_c$  is the current joint angle,  $\beta$  is a positive number smaller than 1 for stability and  $\Delta\theta_{max}$  is a small amplitude compatible with the small variation hypothesis.

The fatigue reduction constraints are managed by hysteresis thresholding which forces a minimal duration for the recovery by setting a lower threshold for de-activating the constraints. The process is iterated to converge toward a fatigue-reducing posture that achieves other user-defined tasks (e.g. reach, balance, etc...).

The fatigue reducing constraint is updated and maintained until a recovery level is achieved. At that point the constraint is deactivated, hence enlarging the solution space for achieving the user-defined tasks.

## 4 RESULTS

In this section we focus on three case of elbow flexion/extension in various body postures: frontal, oblique and lateral upper arm. In all cases, the initial posture is due to a position task achieved by Inverse Kinematics. This task leads to the emergence of fatigue until a critical level that triggers the fatigue reduction constraint (Rodríguez, 2004). We especially examine the convergence behaviour resulting from the iterative hybrid active torque minimization until the active torque is effectively reduced. This behaviour depends on the strategy type *active* vs *passive* (see section 2.1) and the user-given decreased ratio  $R_{\min}$  (see section 2.2). The active torque (yellow curve) is iteratively minimized from an *initial posture* (black point) towards a final one where a *goal with reduced active torque* (green point) is achieved.

It is important to recall that in the three studied cases the external torque is induced by the gravity, and the only joint that moves is the elbow. This allows to draw the external torque function (i.e. the red curve on Figure 1, Figure 10 and Figure 12), however only the local knowledge of the external torque is exploited in the following results.

### 4.1 Horizontal upper arm

The algorithm case 3.2 is first iteratively executed in Figure 7 for an *active* strategy with  $R_{\min}=1$ . The resulting choice provided by the algorithm is however a passive solution for the elbow because the desired 100% reduction of the active torque cannot be achieved in the mid-range of the joint from the extrapolation of the rather flat external torque slope (see Figure 1). As the active torque is positive ( $\tau_c$  is below the  $-\tau_p(\theta)$  curve), a dichotomic search is done between  $\theta_{\min}$  and  $\theta_{s_{\min}}$ . After some iterations executing case 3.2, the case 2.1 is executed as the joint active torque is becoming smaller than  $\epsilon_\tau$  (i.e. the current external torque is between the two small dotted curves shown in Figure 2). As the current state is close to the limit region and the active torque does not change sign between  $\theta_{s_{\min}}$  and  $\theta_{s_{\max}}$ , the algorithm keeps the current state as goal state (see Figure 4a). In addition, the convergence illustrated in Figure 7 is also obtained for a passive strategy.

In Figure 7 and Figure 9 there is a discontinuity at the end of the convergence towards the goal; this is due to the use of a reshaped passive torque function. It is done via the inclusion of two linear terms close to both joint extremes. It ensures that, for

extreme passive solutions, passive torque value is big enough to compensate external torque.

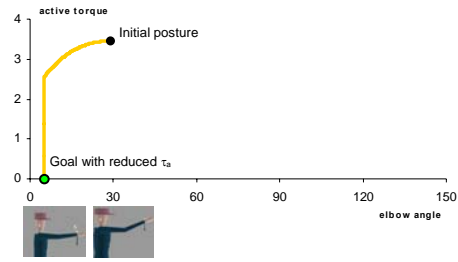


Figure 7. 1)  $R_{\min}=1$  and *active* strategy 2) *passive* strategy. Algorithm's cases 3.2 and 2.1 are successively executed

In Figure 8 the strategy is also *active* but the given minimal reduction ratio,  $R_{\min}$ , is much smaller with a value of 0.2. So it is possible to find a mid-range solution where at least a 20% of active torque reduction is achieved. The case 3.1 is first executed, the goal angle being defined by  $\theta_{\tau_a_{\min}}$  which value for a positive active torque is  $\theta_{s_{\max}}$  (i.e.  $\tau_c$  is below the  $-\tau_p(\theta)$  curve). After some iterations, the case 3.3 is executed owing to the large derivative of the external torque (i.e. the line  $\tau_c(\theta)$  crosses the  $-\tau_p(\theta)$  curve). The continuity of the provided solution is preserved by the algorithm as the solution returned by the dichotomic search between  $\theta_{s_{\min}}$  and  $\theta_{s_{\max}}$  is close to  $\theta_{s_{\max}}$  given by the previous searches. Finally, case 2.1 is executed when  $\tau_a$  becomes smaller than  $\epsilon_\tau$ .

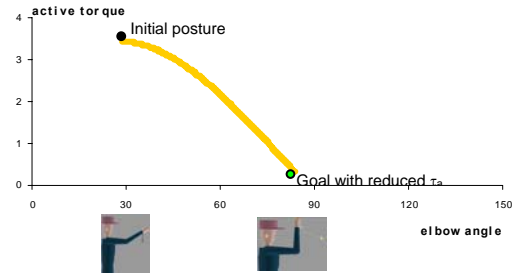


Figure 8.  $R_{\min}=0.2$  and *active* strategy. Algorithm's cases 3.1, 3.3 and 2.1 are successively executed

The passive strategy adopted in Figure 9 and the active torque sign change between  $\theta_{s_{\min}}$  and  $\theta_{s_{\max}}$  (see Figure 5b), lead to execute case 3.4 which returns the first passive solution in the direction of torque active decreasing amplitude, i.e. close to the upper limit. During the last iterations the case 2.3 is

executed when  $\tau_a$  becomes smaller than  $\epsilon_\tau$ , which maintains the current extremal/passive solution.

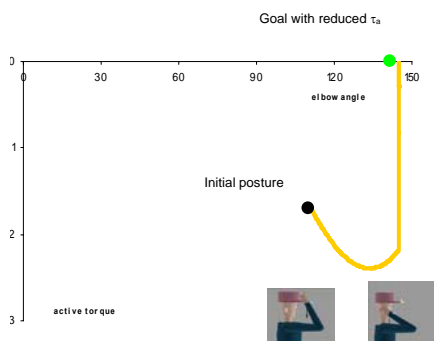


Figure 9. *Passive* strategy. Algorithm's cases 3.4, and 2.3 are successively executed

### 4.2 Oblique upper arm

Figure 11 shows the only solution obtained by simulations for different combinations of parameters (strategy *active* or *passive*,  $R_{min}=1$  or  $R_{min}=0.2$ ). Note how it coincides with the solution given by the particular study depicted in Figure 10.

During the first iterations, the small positive external torque slope leads to execute the case 3.2 because the active torque does not change sign and it is positive. Then the solution is given by dichotomic search between  $\theta_{min}$  and  $\theta_{s\_min}$ . During the last iteration, when the active torque has been reduced under  $\epsilon_\tau$ , the case 1.1 is executed, returning as solution the current angle, due to the negative values of external torque slope and, in consequence, the failure in the search slope (no angle where  $d\tau_p = -d\tau_e$ ).

### 4.3 Lateral with oblique upper arm

This case study is shown in Figure 12. A simulation using  $R_{min}=1$  and *active*, or *passive* strategies (see Figure 13), returns a *passive* solution as depicted in the previously described oblique upper arm case study (firstly case 3.2 is executed, and finally case 1.1).

Using  $R_{min}=1$  and *active* strategy is illustrated on Figure 14 in the other side of the joint range. The external torque slope is large and case 3.3 is executed because  $\tau_e$  crosses the  $-\tau_p(\theta)$  curve, then an *active* solution is found when a dichotomy search between  $\theta_{s\_min}$  and  $\theta_{s\_max}$  is performed. Finally, case 2.1 is executed.

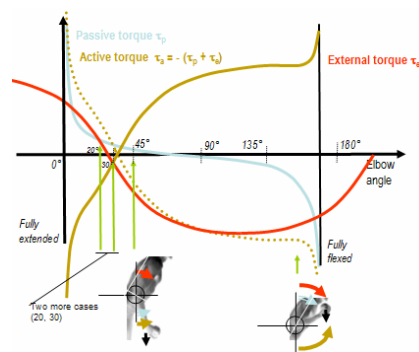


Figure 10. Oblique upper arm case study

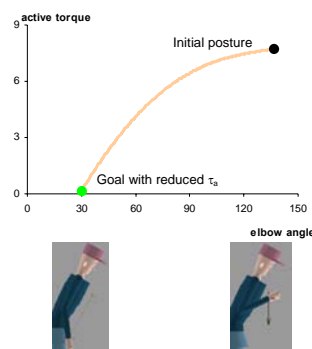


Figure 11.  $R_{min}=1$  or 0.2 and active or passive strategies. Algorithm's cases 3.2 and 1.1 are successively executed

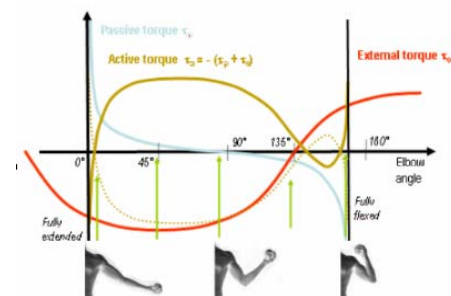


Figure 12. Lateral with oblique upper arm case study

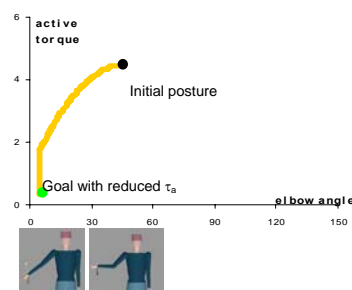


Figure 13.  $R_{min}=1$  and active or passive strategies. Algorithm's cases 3.2 and 1.1 are successively executed

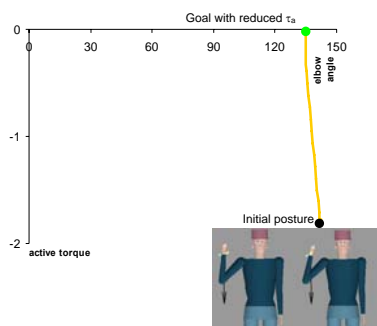


Figure 14.  $R_{\min}=1$  and active. Algorithm's cases 3.3 and 2.1 are successively executed

## 5 DISCUSSION

The main contribution of this paper is a general and hybrid algorithm that clearly delineates all the cases where a solution can be found in the direction reducing the active torque amplitude (*active* strategy) or in the direction of the always existing passive-resistive solution. We don't use a minimization technique like gradient descent as it exploits local knowledge of external and passive torque and cases where the derivative is null provide no solution. Our approach can infer from the current state whether it is possible or not to find an *active* solution. In case it is not possible the *passive* solution is provided.

The algorithm only makes the small assumption that the passive-resistive torque function is a monotonously decreasing function over the joint range. We have also introduced a user-given parameter named the minimal active torque decrease ratio  $R_{\min}$  that leads to accept a partial decrease in the active torque amplitude compatible with the fatigue recovery.

The active torque reduction scheme is exploited in a constrained Inverse Kinematics framework that adjusts automatically fatigued postures while trying to achieve a set of constraints representing a task (Rodríguez, 2004). The exploited fatigue model has been described in (Rodríguez et al., 2002).

Our future work includes the extension of the case studies to those involving several joints, possibly fatigued. For example, this will allow to generate a wide range of standing poses, including the pelvic slouch or contraposto. In addition we plan to take advantage of the environment to have rest. For example, when arm joints are too fatigued, a postural change could employ objects in the scene (a chair, a table) to find rest.

## REFERENCES

- Baerlocher P., Boulic R., 2004. An Inverse Kinematic Architecture Enforcing an Arbitrary Number of Strict Priority Levels, *The Visual Computer*, Springer, 20(6)
- Craig, J., 1986. Introduction to robotics : Mechanics and control , *Addison-Wesley*
- S. Delp, P. Loan, M. Hoy, F. Zajac, S. Fisher, J. Rosen., 1990. An Interactive Graphics-based Model of the Lower Extremity to Study Orthopaedic Surgical Procedures. *IEEE Transactions on Biomedical Engineering*, 37(8):757-767
- Esteki A, *Mansour JM*, 1996. An Experimentally Based Nonlinear Viscoelastic Model of Joint Passive Moment. *Journal of Biomechanics*, 29(4):443-450
- Evans P., 1979. The Postural Function of the Iliotibial Tract. *Royal College of Surgeons*. 61:271-280.
- Giat Y, Mizrahi J, Levy M., 1993. A Musculotendon Model of the Fatigue Profiles of Paralyzed Quadriceps Muscle under FES. *IEEE Tran. on Biomedical Engineering*, 40(7):664-674
- Hatze H., 1997. A three-dimensional multivariate model of passive human joint torques and articular boundaries, *Clinical Biomechanics* 12, 128-135 Institute of Technology, 1998. 3, 4
- Komura T, Shinagawa Y, 2001. Attaching Physiological Effects to Motion-Captured Data. *Graphics Interface Proceedings*, 27-36
- Kulig K., Andrews J. G., Hay J., 1984. Human Strength Curves. In *RJ Terjung (ed) exercise sport science reviews*, 417-466. Lexington MA, DC Heath.
- Kumar P., 1986. Influence of Posture on Muscle Contraction Behaviour in Arm and Leg *Ergometry. The Ergonomic of Working Postures*, ch. 16. Taylor and Francis.
- Manenica I., 1986. A Technique for Postural Load Assessment. *The ergonomics of Working Postures*, Taylor&Francis, London, 271-277
- Multon F., 1988. Biomedical simulation of human arm motion. *Proceedings of the 12th European Simulation Multiconference on Simulation - Past, Present and Future* 305 - 309. ISBN: 1-56555-148-6.
- Rodríguez I, 2004. Joint level fatigue simulation for its exploitation in human posture characterization and optimization. *PhD. Thesis*, University of Alcalá.
- Rodríguez I, Boulic R, Meziat D., 2002. A Joint-Level Model of Fatigue for the Postural Control of Virtual Humans. *Human and Computer*, 220-225. Tokyo